Article

Progress of Multiwalled Carbon Nanotubes for Controlling in Dielectric Characterization of Silicone Rubber

Ahmed Thabet[1]* and Fahad. A. Almufadi[2]

[1] *Nanotechnology Research Center, Electrical Engineering Dept., Faculty of Energy Engineering, Aswan University, Egypt;* athm@aswu.edu.eg

[2] *Qassim University, Department of Mechanical Engineering, College of Engineering, Buraydah 51452, KSA;* almufadi@qec.edu.sa

* Correspondence: athm@aswu.edu.eg

Abstract: Multiwalled Carbon Nanotubes (MWCNTs) is more efficient for fabrication modern design of silicone rubber (SR) that used in industrial engineering applications; it has been embedded in room temperature vulcanization silicone rubber (RTV-SR) matrix for controlling in dielectric characterization. Frequency dielectric measurements were performed for multiwalled carbon nanotubes SR/MWCNT nanocomposites. Hence, the dielectric properties of modern design SR/MWCNT nanocomposites has been deduced as experimental work done to clarify the benefit of filling MWCNT with different patterns inside dielectrics. In variant thermal conditions (up to 40°C), it has been investigated that the new behaviors of SR/MWCNT nanocomposites dealing with nanotechnology techniques for designing new dielectric behaviors of insulation materials. Finally, this research succeeded to characterize dielectric constant, electric modulus and dielectric loss of SR/MWCNT nanocomposites with respect to traditional silicon rubber under variant thermal conditions and frequency response analysis (FRA) according to using certain types and concentrations of MWCNTs.

Keywords: Silicone rubber; Multiwalled Carbon Nanotubes; Sensors; Dielectric properties; Thermal conditions; Nanocomposites.

1. Introduction

Carbon nanotubes define the dielectric properties of polymer nanocomposites, electrical conductivity of the carbon nanotubes, its aspect ratio, as well as dispersion in the polymer. The sensor is one of the potential applications of polymer nanocomposites having carbon nanotubes. The dielectric loss can be determined from the measurements of their dielectric properties such as complex permittivity, ac and dc electrical conductivities, impedance, and tan loss. Nanofillers such as carbon nanotubes (CNTs) have risen as a promising alternative to the high amount of carbon black that is required to obtain optimum reinforcing properties [1]. CNTs at low percentage content provide high mechanical and electrical properties that carbon black provides at high filler content [2]. Therefore, CNT are often used as a reinforcing nanofiller to improve the properties of polymer composites [3,4]. The incorporation of CNT nanofillers significantly improves the mechanical and electrical properties of rubber nanocomposites [5]. However, the use of a high amount of CNT may lead to lower properties due to CNT aggregation in the rubber matrix [6,7]. Significant progress is also being made in CNT dispersion, processing, and their use in silicone rubber. Solution mixing is preferred as it leads to uniform dispersion of CNT in a silicone rubber matrix [8]. Studies report that the reinforcement of silicone rubber with CNT hybrid fillers leads to higher electrical sensitivity [9]. The effect of the purity of CNT in silicone rubber was also studied, and the results show that CNT with high chemical purity show higher mechanical and electrical properties [10]. In recent years, dielectric materials have

Preprints (www.preprints.org) | NOT PEER-REVIEWED | Posted: 5 May 2023 doi:10.20944/preprints202305.0336.v1

attracted a great attention on account of their potential applications such as electric energy storage devices, dielectric actuators, and sensors. to name a few. The feature of dielectric materials is to transmit, store, and record the effects of electricity in the form of electric polarization, that is, electric field induced separation and alignment of electric charges. As the real application of dielectric materials, dielectric constant, and dielectric loss are the two main points focused as the large dielectric constant and low dielectric loss are demanded [11-16]. It has been cleared that Polymers are typically immiscible and usually acquire a small-scale arrangement of the phases when mixed together because of the unfavorably low mixing entropy. "Double percolation" formed by co-continuous structure of immiscible polymer system has been investigated to achieve higher electrical conductivity with reduced conductive filler content "carbon nanotubes" and decreased percolation threshold [17–22]. Thus, this paper has been studied dielectric properties of silicon rubber in presence of carbon nanotubes with variant thermal conditions (up to 40oC). In this study, the effect of carbon nanotubes (CNTs) on the microstructure, electrical conductivity and relative dielectric permittivity of silicon rubber nanocomposites were investigated with variant thermal temperatures over all frequencies up to 1kHz. The proposed experiment samples take into account the different between tradition silicon rubber and the new SR/MWCNT nanocomposites that are used as sensors applications. Also, this research success for specifying optimal dielectric properties of variant thermal conditions for enhancing polymeric insulations for sensors applications. It has been investigated dielectric properties (dielectric constant, modulus, dielectric loss)) with variant thermal temperatures over all frequencies up to 1kHz. Virgin and compressed samples explain the operation state of materials before and after usage for a long-life time.

2. Characterization and Material Design

Polymer composites with CNTs investigated in recent research exhibited improved thermal stability, and thus some research aiming to clarify the mechanism of the improvement by CNTs has been conducted [26–28]. In recent years, dielectric response technology has attracted more and more attention as a non-destructive test method on insulating materials. The polarization and depolarization current (PDC) measurement in time-domain is especially suitable for the on-field diagnosis of electrical equipment because of its fast, accurate and abundant test information [29-33].

2.1 Nanostructure Materials

Monitoring of structures constantly for crack initiation and propagation is a critical issue for reducing inspection costs and increasing safety. The MWCNTs (procured from Nanostructured and Amorphous Materials, Inc. USA) used with RTV-SR are relatively short (10–50 _m), 8-15 nm diameter (density 2.1 g/cm3), with surface area 230 m2/g (> 95% purity) less tangled, and quite straight. In this research, the maximum MWCNT's loading was limited to3.0 wt.% (2.16 vol%) of MWCNT in liquid SR. Two component silicone elastomer which cures at room temperature by a poly addition reaction (commercially known as BLUESIL RTV 3428 A&B) is used as received. The density of both SR component is 1.1 g/cm3whereasthe viscosities of RTV-A and RTV-B are 25,000 and 8000 mPa.s, respectively. At low CNT concentrations in the nanocomposite, large conductivity fluctuations may occur due to the strong influence of destruction and formation of conductive paths [23]. When using MWCNTs, the main problem is their characteristic property of agglomeration due to their physical size and the van-der Waals forces between the nano particles. Using surfactants (e.g., poly carboxylic acid or sodium dodecylbenzene sulfonate NaDDBS) and low-power, high-frequency (12 W, 55 kHz) sonication for 16 − 24 h is required to achieve MWCNTs dispersion in polymer, which are normally very elaborate and complicated. The SR/MWCNT nanocomposite samples are prepared according to the weight percent (wt.%) of the MWCNTs and SR. The samples are produced by melt-mixing of MWCNTs with SR without surfactants using a laboratory mixer with a high shear mixing blade. The tendency of MWCNTs agglomerations in polymer matrix may be minimized by appropriate application of shear during the melt-mixing [24, 25]. It is shown that a good dispersion and wetting of the MWCNTs can be achieved with RTV polymer by the shear mixing. It is useful to mention that the

Preprints (www.preprints.org) | NOT PEER-REVIEWED | Posted: 5 May 2023 doi:10.20944/preprints202305.0336.v1

viscosity of the mixture increases with the increasing wt.% of the carbon nanotubes. When MWCNTs are visibly wetted-out, the mixing speed is gradually increased until the mixture exhibits no visible signs of lumps. After 4 min of cooling, RTV-B is added and mixed at low speed for two minutes. The SR/MWCNT blend is then poured into molds with different forms according to the desired shape and size of the flexible sensor.

2.2 Fabrication Materials

The high electrical, dielectric and mechanical properties have been improved in thermal conditions and thermal stability with attractive of high-performance CNTs. The MWCNT's dispersion inside the cured RTV (rubber silicone) is examined by SEM using a FEI-Apreo Electron Microscope, operating at 2.0 and 20 kV. The SR/MWCNT samples are prepared to SEM investigation by immersing small trimmed pieces from molded blocks (dimensions 5 × 5 × 2 mm) in liquid nitrogen at room temperature and then fracturing the frozen pieces laterally into two pieces such that the fracture surface is perpendicular to the electric current direction to show the SR/MWCNTs phase and the RTV polymer phase. The morphology of the cross-section area of this fractured piece in Fig. 1(a) shows how the carbon nanotube networks are embedded within the silicon rubber matrix. The shapes of the nanotubes. SEM image in Fig. 1(b) shows the morphology of the SR/MWCNTs sample at higher magnification to show the uniform spatial distribution of individual MWCNTs that result in the high conductivity of the SR/MWCNT nanocomposites. One of the two fractured pieces is fractured again in a direction perpendicular to the first fractured cross section area to reveal the convolution, entanglement and the degree of alignment of MWC- NTs within the conductive networks in the SR as shown in Fig. 1(c); The explored area reveals the well dispersion and the high density of the MWCNTs conductive networks within the polymer matrix.

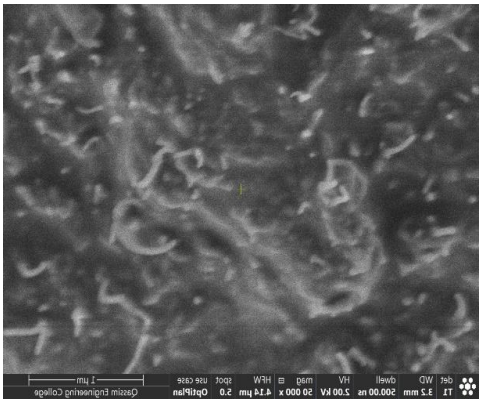

(a) SEM image for cross section (50,000x)

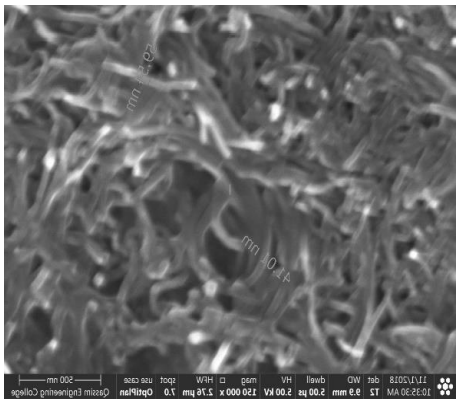

(b) SEM image for conductive networks (150,000x)

Preprints (www.preprints.org) | NOT PEER-REVIEWED | Posted: 5 May 2023 doi:10.20944/preprints202305.0336.v1

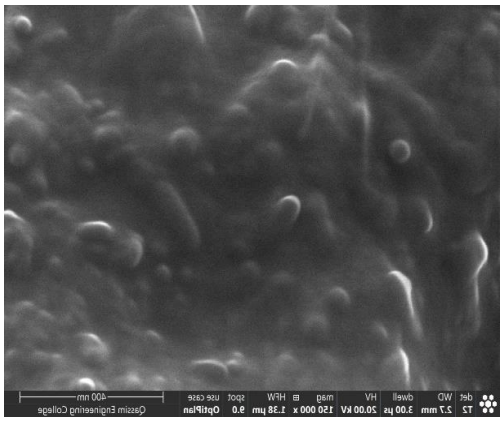

(c) SEM image of conductive networks at fracture surface at high magnification (120,000×).

Figure 21. SEM images MWCNTs-RTV nanocomposites.

2.3 Fabrication Test Samples

Fabrication prototypes of nanocomposite samples are made either by slicing or trimming of the desired shapes and sizes from the SR/MWCNT molded block or directly by molding the desired shape and size of the RTV. Fig. 2(a) shows different shapes and dimensions of sliced and trimmed SR/MWCNT samples from molded block B. The dimensions of trimmed sensors in Fig. 2(b) range from 1 × 2 x 12 mm (it can be used as strain sample for axial tension) to 4 × 4 x 12 mm (it can be used as bending force sample).

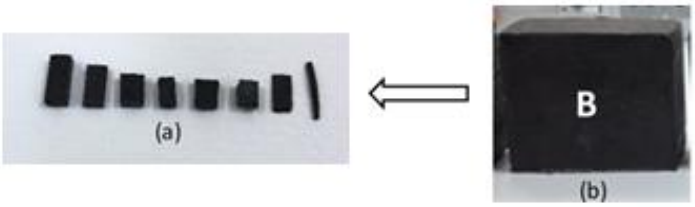

(a) Sliced and trimmed shapes and sizes (b) SR/MWCNT molded block,

Figure 2 Prototypes of RTV sliced or trimmed from molded block B.

3. Characterization & Measurements

Dielectric Spectroscopy is a powerful experimental method to investigate the dynamical behavior of a sample through the analysis of its frequency dependent dielectric response. This technique is based on the measurement of the capacitance as a function of frequency of a sample sandwiched between two electrodes. The resistance (R), inductance (L) and capacitance [C] were measured as a function of frequency in the range of 0.1 Hz to 1 MHz at variant temperatures for all the test samples. HIOKI 3522-50 LCR Hi-tester device has been measured characterization of Silicon rubber/CNTs nanocomposite sensor materials, it has been used for measuring electrical parameters of nanometric sensors specimens at various frequencies. Specification of LCR is Power supply: 100 V, 120 V, 220 V or 240 V (_10 %) AC (selectable), 50/60 Hz, and Frequency: DC, 1 MHz to 100 kHz, Display Screen: LCD with backlight / 99999 (full 5 digits), Basic Accuracy: Z: 0:08 % rdg.: 0:05, and External DC bias _40 Vmax. (option) (3522-50 used alone _10 V max./ using 9268 _ 40 V max.). It can be varied thermal conditions of the specimens with respect to high digital oven (20oC up to 100°C).

 doi:10.20944/preprints202305.0336.v1

4. Results and Discussion

The role of matrix viscosity and type of nanotubes on the dielectric and conductivity that has been explained reinforced with SR/MWCNT nanocomposites samples. It has been observed that the shape of the nanotubes and viscosity of the matrix influenced the magnitude of dc conductivity at percolation threshold, whereas the ac conductivity keeps on increasing with increasing fill loading in all matrices.

4.1 Characterization of Traditional Silicon Rubber Samples

The dielectric characterization of the tested samples (virgin and compressed) is shown in Figure 3(a, b) as a function of frequency for Silicon rubber at variant thermal temperatures (up to 40oC). The measured real dielectric constant in Figure 3(a) contrasts on increasing real part of dielectric constant with increasing thermal temperatures, whatever, there is a slight increasing via increasing frequency up to 10Hz but decreasing is done via increasing frequency. Also, Fig. 3(b) clarifies that a reduction of the real dielectric constant of compressed silicon rubber samples versus variant thermal temperatures (up to 40oC) with respect to virgin samples, whatever, there is a slight increasing via increasing frequency up to 10Hz but decreasing is done via increasing frequency. Analysis of imaginary dielectric constant characterization can be shown in Fig. 4(a, b) that shows the imaginary part of dielectric constant of the tested samples (virgin and compressed) as a function of frequency for Silicon rubber at variant thermal temperatures (up to 40oC). The measured imaginary dielectric constant in Figure 4(a) contrasts on a closed increasing imaginary part of dielectric constant with increasing thermal temperatures, whatever, there is a slight increasing via increasing frequency up to 10Hz but decreasing is done via increasing frequency. Also, Fig. 4(b) clarifies that a closed reduction of the real dielectric constant of compressed silicon rubber samples versus variant thermal temperatures (up to 40oC) with respect to virgin samples, whatever, but there is a slight increasing via increasing frequency up to 10Hz but decreasing is done via increasing frequency.

Preprints (www.preprints.org) | NOT PEER-REVIEWED | Posted: 5 May 2023 doi:10.20944/preprints202305.0336.v1

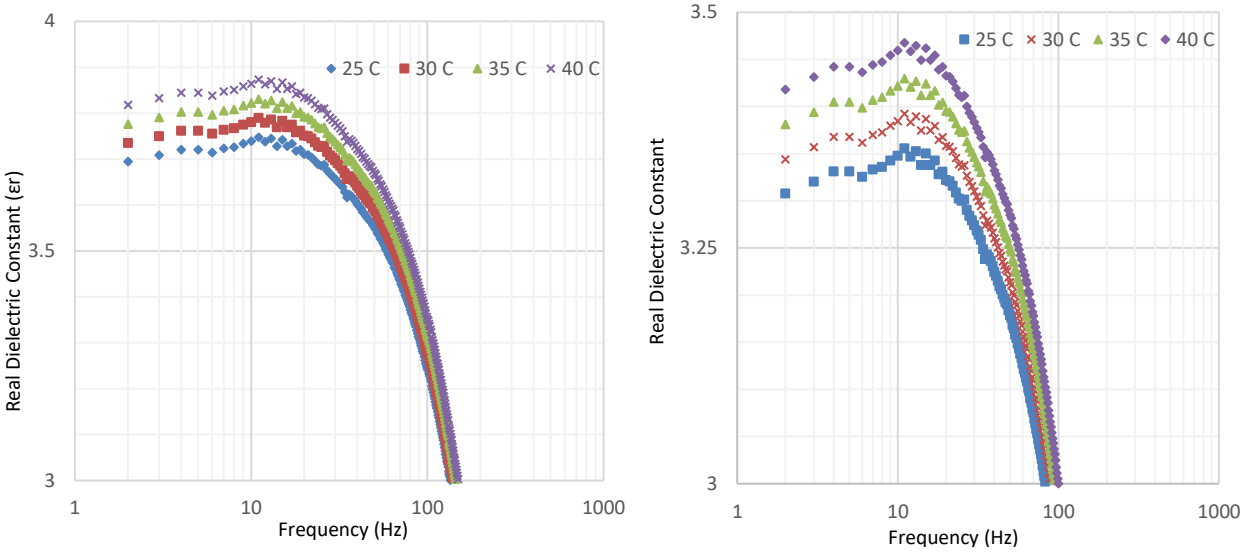

(a)Virgin Sample (b) Compressed Sample

Figure 3 Real dielectric constant of SR under variant frequencies and thermal conditions

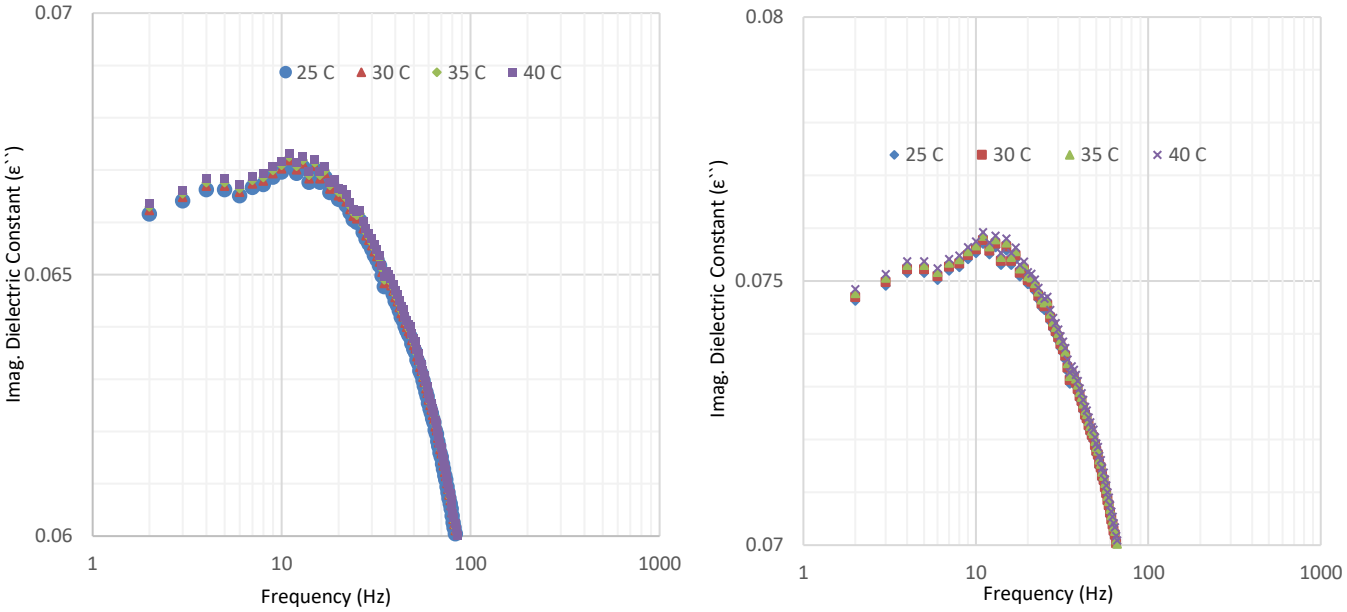

(a)Virgin Sample (b) Compressed Sample

Figure 4 Imaginary dielectric constant of SR under variant frequencies and thermal conditions

Preprints (www.preprints.org) | NOT PEER-REVIEWED | Posted: 5 May 2023 doi:10.20944/preprints202305.0336.v1

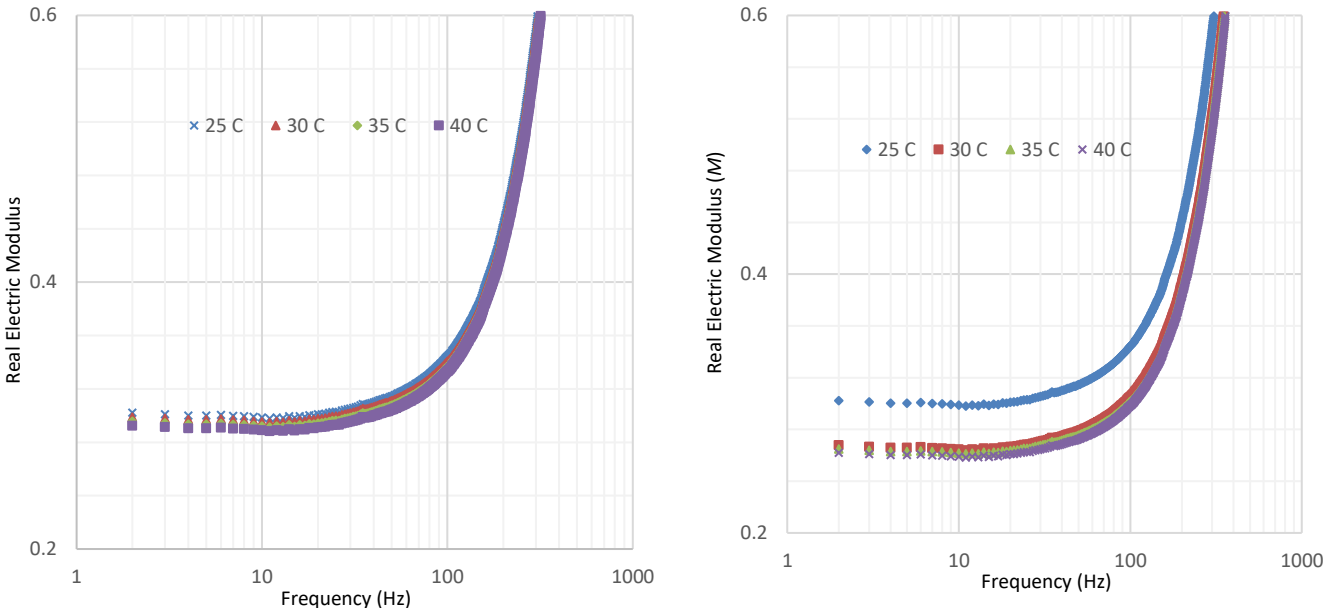

(a)Virgin Sample (b) Compressed Sample

Figure 5 Real electric modulus of SR under variant frequencies and thermal conditions

Real electric modulus characterization is shown in Fig. 5(a, b) for the tested samples (virgin and compressed) as a function of frequency for Silicon rubber at variant thermal temperatures (up to 40°C). The measured real electric modulus in Fig. 5(a) contrasts on decreasing real electric modulus with increasing thermal temperatures; whatever, fixation real electric modulus values occur at low frequencies (up to 100Hz) but increasing the real electric modulus happened at high frequencies (More than 100Hz). On the other hand, Fig. 5(b) clarifies the decreasing in real electric modulus values for compressed silicon rubber samples with respect to the same performance of virgin samples at variant thermal temperatures (up to 40°C) over all frequencies. On the other hand, imaginary electric modulus characterization is shown in Fig. 6(a, b) that clarifies the electric modulus of the tested samples (virgin and compressed) as a function of frequency for Silicon rubber at variant thermal temperatures (up to 40oC). The measured imaginary electric modulus in Fig. 6(a) contrasts on decreasing imaginary electric modulus with variant thermal temperatures; whatever, a closed increasing imaginary electric modulus values occurs at low frequencies (up to 100Hz) but the increasing the imaginary electric modulus is happened at high frequencies (More than 100 Hz). Also, Fig. 6(b) clarifies the decreasing in imaginary electric modulus values of compressed silicon rubber samples with respect to the same performance of virgin samples versus frequency at variant thermal temperatures (up to 40°C).

Preprints (www.preprints.org) | NOT PEER-REVIEWED | Posted: 5 May 2023 doi:10.20944/preprints202305.0336.v1

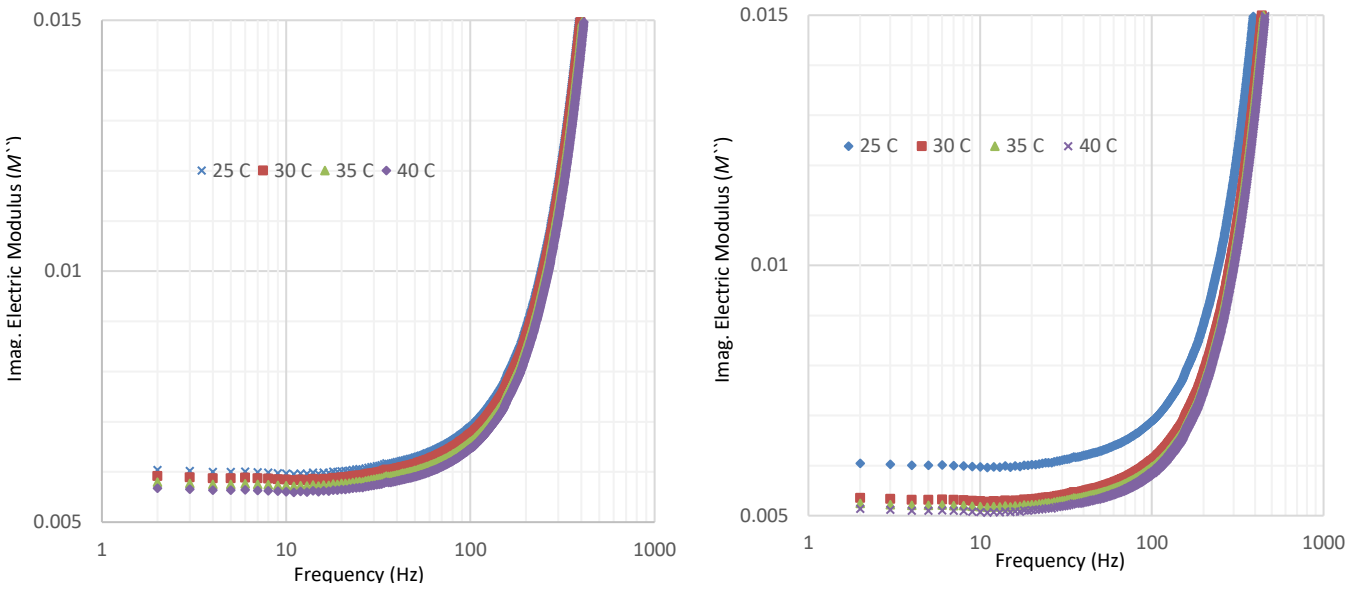

(a)Virgin Sample (b) Compressed Sample

Figure 6 Imaginary electric modulus of SR under variant frequencies and thermal conditions

4.2 Characterization of MWCNTs

The dielectric characterization of the tested samples (virgin and compressed) is shown in Figure 7(a, b) as a function of frequency for SR/MWCNT nanocomposites at variant thermal temperatures (up to 40oC). The measured real dielectric constant in Figure 7(a) contrasts on decreasing real part of dielectric constant with increasing thermal temperatures, whatever, there is decreasing via increasing frequency up to 1kHz. Also, Fig. 7(b) clarifies that a reduction of the real dielectric constant of compressed SR/MWCNT nanocomposites samples versus variant thermal temperatures (up to 40oC) with respect to virgin samples, whatever, there is decreasing the real dielectric constant via increasing frequency up to 1kHz. Analysis of imaginary dielectric constant characterization can be shown in Fig. 8(a, b) that shows the imaginary part of dielectric constant of the tested samples (virgin and compressed) as a function of frequency for SR/MWCNT nanocomposites at variant thermal temperatures (up to 40oC). The measured imaginary dielectric constant in Figure 8(a) contrasts on decreasing imaginary part of dielectric constant with increasing thermal temperatures, and so, there is decreasing via increasing frequency up to 1kHz. On the other hand, Fig. 8(b) clarifies that excess of the imaginary dielectric constant of compressed SR/MWCNT nanocomposites samples versus variant thermal temperatures (up to 40oC) with respect to virgin samples, whatever, but there is decreasing via increasing frequency up to 1kHz.

Preprints (www.preprints.org) | NOT PEER-REVIEWED | Posted: 5 May 2023 doi:10.20944/preprints202305.0336.v1

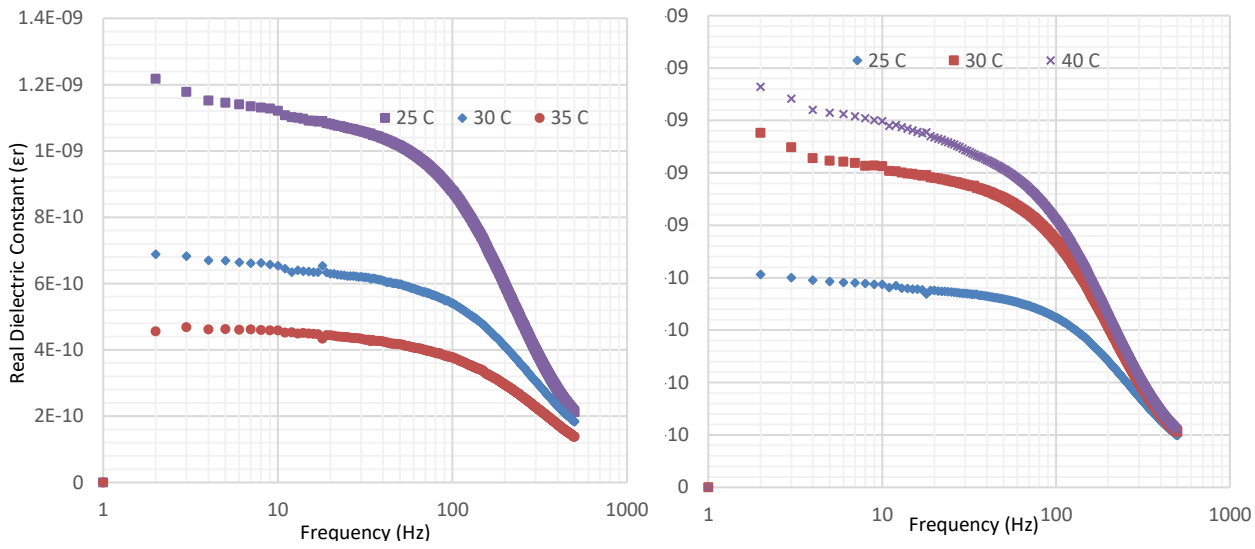

(a)Virgin Sample (b) Compressed Sample

Figure 7 Real dielectric constant of SR/MWCNT nanocomposites under variant frequencies and thermal conditions

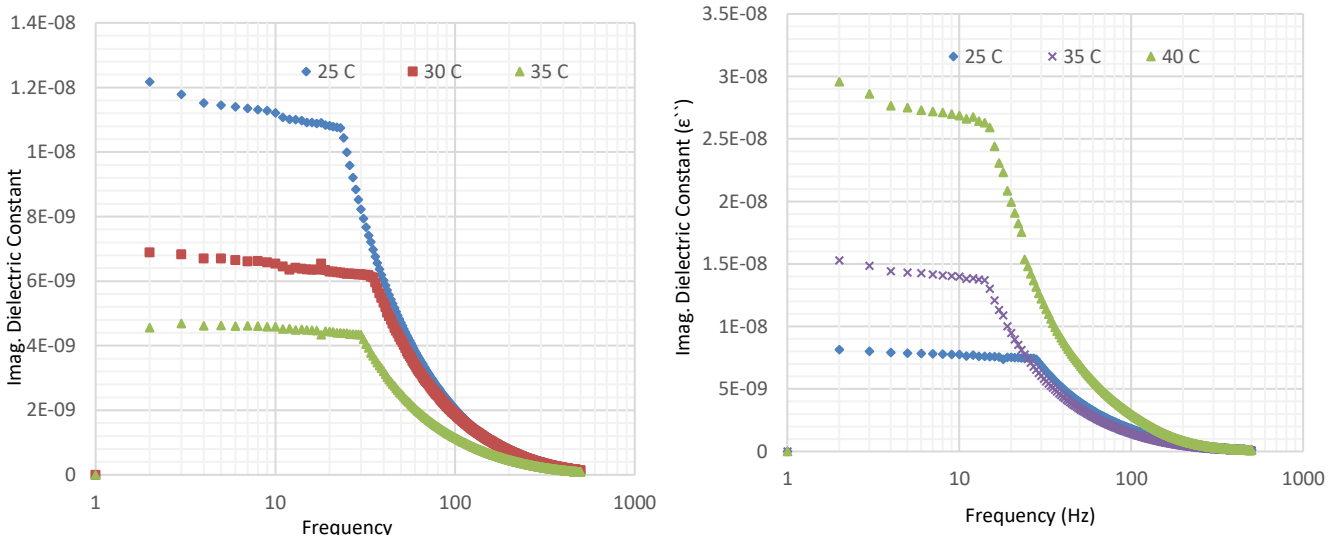

(a)Virgin Sample (b) Compressed Sample

Figure 8 Imaginary dielectric constant of SR/MWCNT nanocomposites under variant frequencies and thermal conditions

Preprints (www.preprints.org) | NOT PEER-REVIEWED | Posted: 5 May 2023 doi:10.20944/preprints202305.0336.v1

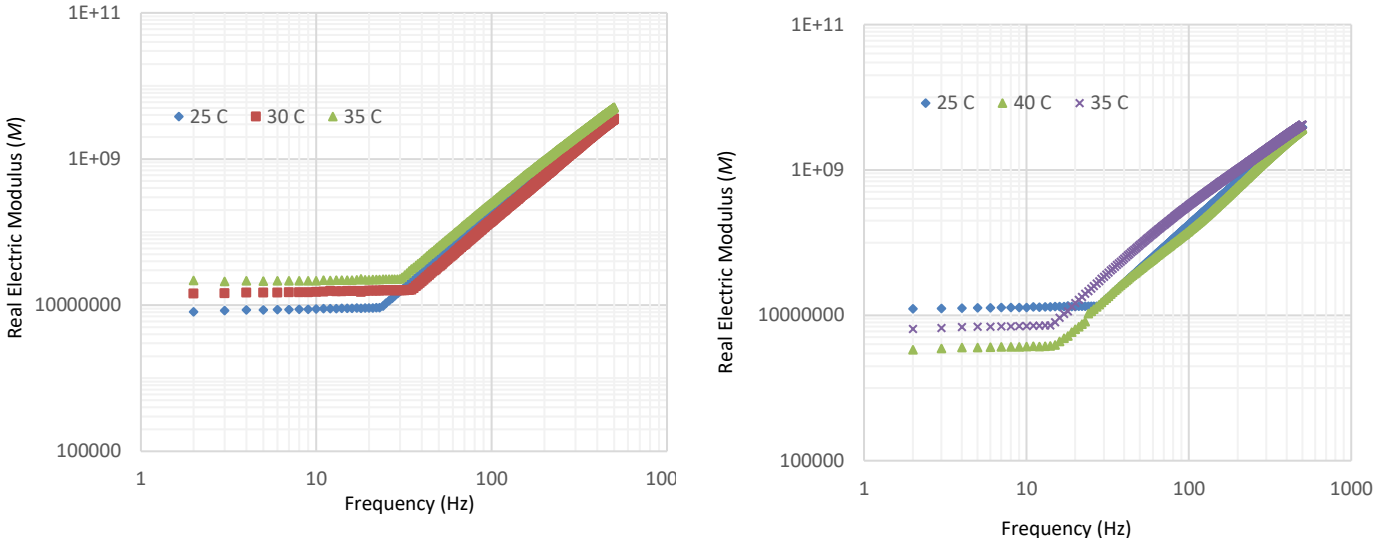

(a)Virgin Sample (b) Compressed Sample

Figure 9 Real electric modulus of SR/MWCNT nanocomposites under variant frequencies and thermal conditions

Real electric modulus characterization is shown in Fig. 9(a, b) that shows the real electric modulus of the tested samples (virgin and compressed) as a function of frequency for SR/MWCNT nanocomposites at variant thermal temperatures (up to 40°C). The measured real electric modulus in Fig. 9(a) contrasts on increasing real electric modulus with increasing thermal temperatures; whatever, fixation real electric modulus values occur at low frequencies (up to 50Hz) but the real electric modulus excess happened at frequencies (More than 50Hz). On the other hand, Fig. 9(b) clarifies the reduction in real electric modulus values of compressed SR/MWCNT nanocomposites samples with respect to the same performance of virgin samples versus frequency at variant thermal temperatures (up to 40oC). On the other hand, imaginary electric modulus characterization is shown in Fig. 10(a, b) that shows the electric modulus of the tested samples (virgin and compressed) as a function of frequency for SR/MWCNT nanocomposites at variant thermal temperatures (up to 40°C). The measured imaginary electric modulus in Fig. 10(a) contrasts on increasing imaginary electric modulus with thermal temperatures; whatever, fixation imaginary electric modulus values occur at low frequencies (up to 50Hz) but increasing the imaginary electric modulus happened at high frequencies (More than 50 Hz). On the other hand, Fig. 10(b) clarifies the reduction occur in imaginary impedance values of compressed SR/MWCNT nanocomposites samples with respect to the same performance of virgin samples over all measured frequencies at variant thermal temperatures except that there is a decreasing imaginary electric modulus with increasing thermal temperatures (up to 40°C).

Preprints (www.preprints.org) | NOT PEER-REVIEWED | Posted: 5 May 2023 doi:10.20944/preprints202305.0336.v1

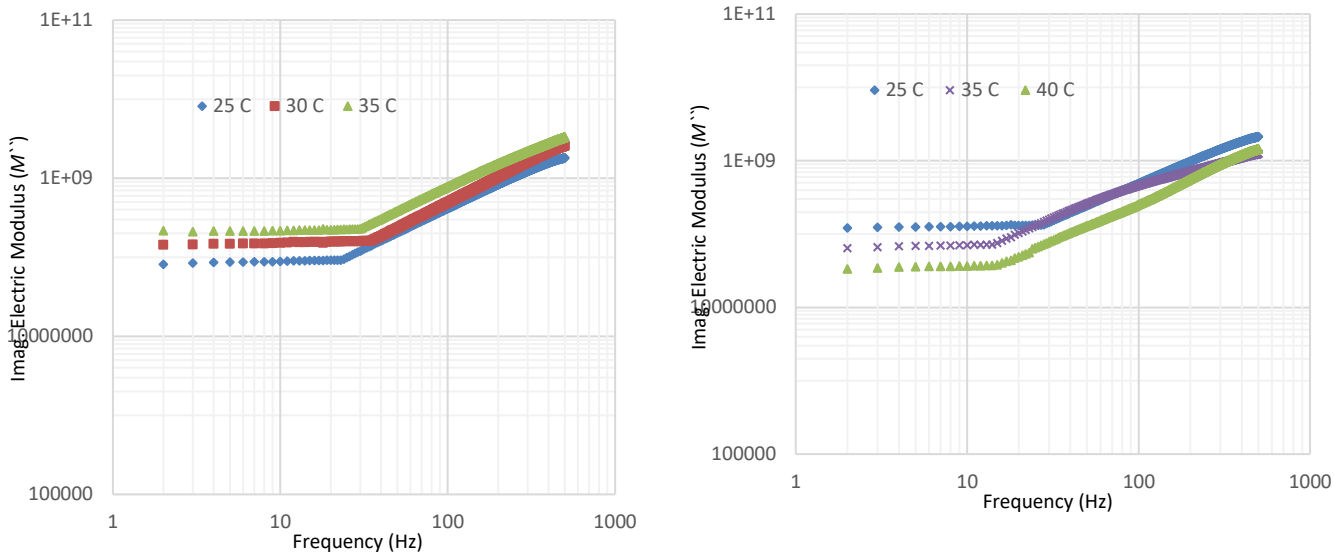

(a)Virgin Sample (b) Compressed Sample

Figure 10 Imaginary electric modulus of SR/MWCNT nanocomposites under variant frequencies and thermal conditions

5. Effect of MWCNTs in Dielectric Loss

Currently, a strong demand comes from electric and dielectric industrial applications, the manufacturing for largest application market for piezoelectric devices, followed by the automotive industry. According to the dielectric loss that quantifies a dielectric material's inherent dissipation of electromagnetic energy, Fig. 11(a, b) has been investigated that the dielectric loss of the tested samples (virgin and compressed) as a function of frequency for silicon rubber at variant thermal temperatures (up to 40oC). The measured dielectric loss in Fig. 11(a) contrasts on decreasing dielectric loss with increasing thermal temperatures; whatever, fixation dielectric loss values occur over all frequencies (up to 1kHz). Also, Fig. 11(b) clarifies that a reduction of the dielectric loss of compressed silicon rubber samples versus variant thermal temperatures (up to 40oC) with respect to virgin samples, whatever, there is fixation the dielectric loss via increasing frequency up to 1kHz. Furthermore, Fig. 12(a, b) shows the dielectric loss characterization of the tested samples (virgin and compressed) as a function of frequency for SR/MWCNT nanocomposites at variant thermal temperatures (up to 40oC). The measured dielectric loss in Fig. 12(a) contrasts on reduction of dielectric loss with increasing thermal temperatures; whatever, fixation dielectric loss values occur at low frequencies (up to 50Hz) but the decreasing of dielectric loss happened at frequencies (More than 50Hz). Whatever, Fig. 12(b) clarifies the reduction occur in dielectric loss values of compressed SR/MWCNT nanocomposites samples with respect to the same performance of virgin samples over all measured frequencies at variant thermal temperatures.

Preprints (www.preprints.org) | NOT PEER-REVIEWED | Posted: 5 May 2023 doi:10.20944/preprints202305.0336.v1

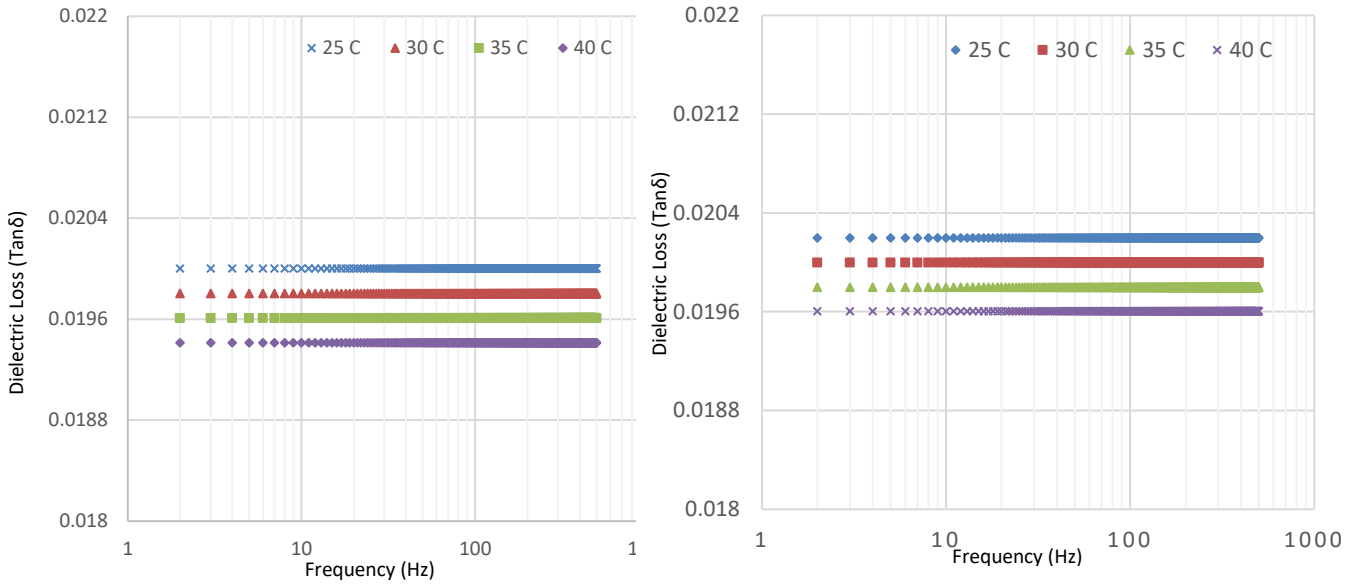

(a)Virgin Sample (b) Compressed Sample

Figure 11 Dielectric loss of SR under variant frequencies and thermal conditions

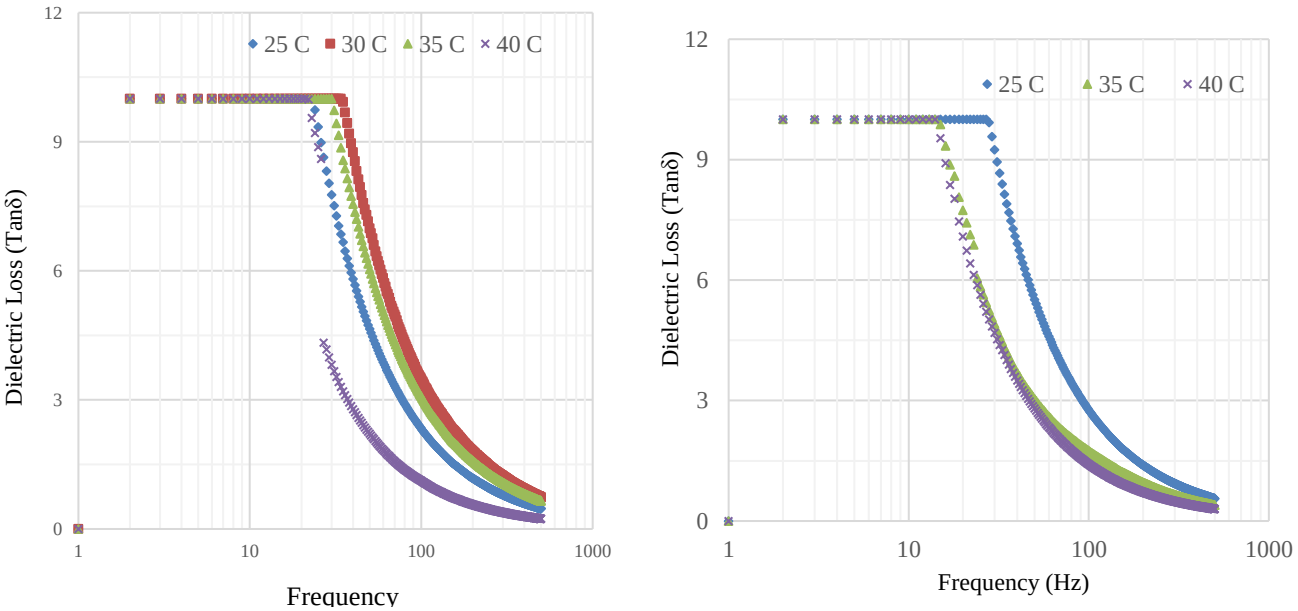

(a)Virgin Sample (b) Compressed Sample

Figure 12 Dielectric loss of SR/MWCNT nanocomposites under variant frequencies and thermal conditions

 doi:10.20944/preprints202305.0336.v1

6. Thermal and Frequency Analysis

In case of pure silicon rubber samples, it is noticed that the measured real dielectric constant focus on increasing real part of dielectric constant with increasing thermal temperatures, whatever, there is a slight increasing via increasing frequency up to 10Hz but decreasing is done via increasing frequency. Also, it clarifies that a reduction of the real dielectric constant of compressed silicon rubber samples versus variant thermal temperatures (up to 40oC) and follow the same behavior with respect to virgin samples. The measured imaginary dielectric constant focus on a closed increasing imaginary part of dielectric constant with increasing thermal temperatures, whatever, there is a slight increasing via increasing frequency up to 10Hz but decreasing is done via increasing frequency. Also, it clarifies that a closed reduction of the real dielectric constant of compressed silicon rubber samples versus variant thermal temperatures (up to 40oC) and follow the same behavior with respect to virgin samples. The measured real electric modulus contrasts on decreasing real electric modulus with increasing thermal temperatures; whatever, fixation real electric modulus values occur at low frequencies (up to 100Hz) but increasing the real electric modulus happened at high frequencies (More than 100Hz). On the other hand, it clarifies the decreasing in real electric modulus values for compressed silicon rubber samples with respect to the same performance of virgin samples at variant thermal temperatures (up to 40oC) over all frequencies. Finally, the measured imaginary electric modulus contrasts on decreasing imaginary electric modulus with variant thermal temperatures; whatever, a closed increasing imaginary electric modulus values occurs at low frequencies (up to 100Hz) but the increasing the imaginary electric modulus is happened at high frequencies (More than 100 Hz). Also, it clarifies the decreasing in imaginary electric modulus values of compressed silicon rubber samples with respect to the same performance of virgin samples versus frequency at variant thermal temperatures (up to 40oC).

In case of SR/MWCNT samples, it is noticed that the measured real dielectric constant focus on decreasing real part of dielectric constant with increasing thermal temperatures, whatever, there is decreasing via increasing frequency up to 1kHz. Also, it clarifies that a reduction of the real dielectric constant of compressed SR/MWCNT nanocomposites samples versus variant thermal temperatures (up to 40oC) with respect to the same performance of virgin samples. The measured imaginary dielectric constant contrasts on decreasing imaginary part of dielectric constant with increasing thermal temperatures, and so, there is decreasing via increasing frequency up to 1kHz. On the other hand, it clarifies that excess of the imaginary dielectric constant of compressed SR/MWCNT nanocomposites samples versus variant thermal temperatures (upto 40oC) with respect to the same performance of virgin samples. The measured real electric modulus focusses on increasing real electric modulus with increasing thermal temperatures; whatever, fixation real impedance values occur at low frequencies (up to 50Hz) but the real impedance excess happened at frequencies (More than 50Hz). On the other hand, it clarifies the reduction in real electric modulus values of compressed SR/MWCNT nanocomposites samples with respect to the same performance of virgin samples versus frequency at variant thermal temperatures (up to 40oC).The measured imaginary electric modulus contrasts on increasing imaginary electric modulus with thermal temperatures; whatever, fixation imaginary electric modulus values occur at low frequencies (up to 50Hz) but increasing the imaginary impedance happened at high frequencies (More than 50 Hz). On the other hand, it clarifies the reduction occur in imaginary impedance values of compressed SR/MWCNT nanocomposites samples with respect to the same performance of virgin samples over all measured frequencies at variant thermal temperatures except that there is a decreasing imaginary electric modulus with increasing thermal temperatures (up to 40oC).

 doi:10.20944/preprints202305.0336.v1

7. Conclusions

This study investigates electrical characterization for conductive SR/MWCNT nanocomposites with different embedded electrical conductors. According to the adopted SR/MWCNT nanocomposites of impact, the material sensitivity depends on the rate of increase of interparticle separation with the impact force. The SR/MWCNT nanocomposites with piezoelectric property can simply be used to fabricate highly sensitive, light weight and small dimensions elastic sensors according to the desired force range.

Experimental tests deduced multiwalled carbon nanotubes (MWC-NTs) are decreasing real part of dielectric constant via increasing thermal temperatures and increasing frequency up to 1kHz. Also, it clarifies that a reduction of the real dielectric constant of compressed SR/MWCNT nanocomposites samples.

It has been deduced that multiwalled carbon nanotubes (MWC-NTs) are decreasing imaginary part of dielectric constant with increasing thermal temperatures, but there is decreasing via increasing frequency up to 1kHz. There is an excess of the imaginary dielectric constant of compressed SR/MWCNT nanocomposites samples.

Multiwalled carbon nanotubes (MWC-NTs) are deduced experimentally the increasing real electric modulus with increasing thermal temperatures; whatever, a reduction in real electric modulus values of compressed SR/MWCNT nanocomposites samples occurs with respect to the same performance of virgin samples.

Experimental tests deduced multiwalled carbon nanotubes (MWC-NTs) are increasing imaginary electric modulus with thermal temperatures; whatever, a reduction occur in imaginary electric modulus values of compressed SR/MWCNT nanocomposites samples with respect to the same performance of virgin samples.

Multiwalled carbon nanotubes (MWC-NTs) are deduced that decreasing of dielectric loss with increasing thermal temperatures; whatever, the reduction occurs in dielectric loss values of compressed SR/MWCNT nanocomposites samples with respect to the same performance of virgin samples over all measured frequencies at variant thermal temperatures.

Acknowledgment

The present work is appreciated the fabrication and SEM observations laboratories in College of Engineering at Qassim University for functional structure preparation SR/MWCNT nanocomposites specimens and so, all greatly appreciation for Nanotechnology Research Center in Faculty of Energy Engineering at Aswan University for research cooperation in dielectric characterization and thermal measurements.

Highlights

Progress dielectric properties of silicon rubber as sensor applications.

Studying stressing SR/MWCNT nanocomposite under variant thermal conditions.

Optimal dielectric characterization of Silicon rubber sensors by using multiwalled carbon nanotubes (MWC-NTs).

layout features of using multiwalled carbon nanotubes (MWC-NTs) for enhancing dielectric Silicon rubber properties.

References

1. Z. Jia, Z. Wang, C. Xu, J. Liang, B. Wei, D. Wu, S. Zhu, Study on poly(methyl methacrylate)/carbon nanotube composites, Mater. Sci. Eng., A 271 (1–2) (1999) 395–400.
2. V. Kumar, D.-J. Lee, Studies of nanocomposites based on carbon nanomaterials and RTV silicone rubber, J. Appl. Polym. Sci. 134 (4) (2017) 44407.

3. R. Andrews, M.C. Weisenberger, Carbon nanotube polymer composites, Curr. Opin. Solid State Mater. Sci. 8 (1) (2004) 31–37.
4. M.H. Al-Saleh, U. Sundararaj, Electromagnetic interference shielding mechanisms of CNT/polymer composites, Carbon 47 (7) (2009) 1738–1746.
5. V. Kumar, G. Lee, Monika, J. Choi, Dong-J. Lee, "Studies on composites based on HTV and RTV silicone rubber and carbon nanotubes for sensors and actuators", Polymer Vol. 190, pp.122221, 2020
6. Q. Yang, X. He, X. Liu, F. Leng, Y. Mai, The effective properties and local aggregation effect of CNT/SMP composites, Compos. B Eng. 43 (1) (2012) 33–38.
7. B. Mathieu, C. Anthony, A. Arnaud, F. Lionel, CNT aggregation mechanisms probed by electrical and dielectric measurements, J. Mater. Chem. C 3 (22) (2015) 5769–5774.
8. V. Kumar, J.-Y. Lee, D.-J. Lee, Synergistic effects of hybrid carbon nanomaterials in room-temperature-vulcanized silicone rubber, Polym. Int. 66 (3) (2017) 450–458.
9. N. Witt, Y. Tang, L. Ye, L. Fang, Silicone rubber nanocomposites containing a small amount of hybrid fillers with enhanced electrical sensitivity, Mater. Des. 45 (2013) 548–554.
10. V. Kumar, D.-J. Lee, Effects of purity in single-wall carbon nanotubes into rubber nanocomposites, Chem. Phys. Lett. 715 (2019) 195–203.
11. Shen Y, Lin YH and Nan CW. Interfacial effect on dielectric properties of polymer nanocomposites filled with core/shell-structured particles. Adv Funct Mater 2007; 17: 2405–2410.
12. G Gallone, F Carpi, DD Rossi, et al. Dielectric constant enhancement in a silicone elastomer filled with lead magnesium niobate-lead titanate. Mater Sci Eng C 2007; 27: 110–116.
13. B Kussmaul, S Risse, G Kofod, et al. Enhancement of dielectric permittivity and electromechanical response in silicone elastomers: molecular grafting of organic dipoles to the macromolecular network. Adv Funct Mater 2011; 21: 4589–4594.
14. SCB Mannsfeld, CKT Benjamin, MS Randall, et al. Highly sensitive flexible pressure sensors with microstructured rubber dielectric layers. Nature Mater 2010; 9: 859–864.
15. Cohen DJ, Mitra D, Peterson K, et al. A highly elastic, capacitive strain gauge based on percolating nanotube networks. Nano Lett 2012; 12: 1821–1825.
16. X. Zheng, Y. Huang, Sh. Zheng, Z. Liu1 and M. Yang, "Improved dielectric properties of polymer-based composites with carboxylic functionalized multiwalled carbon nanotubes", Journal of Thermoplastic Composite Materials, Vol. 32, Issue 4, pp.1-14, 2018,
17. E. Jalali Dil, M. Arjmand, I. Otero Navas, U. Sundararaj, B.D. Favis, Interface bridging of multiwalled carbon nanotubes in polylactic acid/poly(butylene adipate-co-terephthalate): morphology, rheology, and electrical conductivity, Macromolecules 53 (22) (2020) 10267–10277.
18. I.O. Navas, M. Arjmand, U. Sundararaj, Effect of carbon nanotubes on morphology evolution of polypropylene/polystyrene blends: understanding molecular interactions and carbon nanotube migration mechanisms, RSC Adv. 7 (85) (2017) 54222–54234.
19. I. Otero Navas, M. Kamkar, M. Arjmand, U. Sundararaj, Morphology evolution, molecular simulation, electrical properties, and rheology of carbon nanotube/ polypropylene/polystyrene blend nanocomposites: effect of molecular interaction between styrene-butadiene block copolymer and carbon nanotube, Polymers 13 (2) (2021).
20. I. Otero-Navas, M. Arjmand, U. Sundararaj, Carbon nanotube induced double percolation in polymer blends: morphology, rheology and broadband dielectric properties, Polymer 114 (2017) 122–134.
21. I.O. Navas, M. Arjmand, U. Sundararaj, Effect of carbon nanotubes on morphology evolution of polypropylene/polystyrene blends: understanding molecular interactions and carbon nanotube migration mechanisms, RSC Adv. 7 (85) (2017) 54222–54234.
22. L. Zhou, Y. Tian, P. Xu, H. Wei, Y. Li, H-X. Peng, F. Qin, "Effect of the selective localization of carbon nanotubes and phase domain in immiscible blends on tunable microwave dielectric properties", Composites Science and Technology 213 (2021) 108919
23. G. Yin, N. Hu, Y. Karube, Y. Liu, Y. Li, H. Fukunaga, et al., A carbon nanotube/polymer strain sensor with linear and anti-symmetric piezo resistivity, Mech. Compos. Mater. Struct. 45 (2011) 1315–1323.
24. P. Potschke, A.R. Bhattacharyya, A. Janke, S. Pege, A. Leonhardt, C. Taschner, et al., Melt mixing as method to disperse carbon Nanotubes intothermoplastic polymers, Fuller. Nanotub. Car. N. 13, 211–224 (2005).
25. H. A. Sherif∗, F. A. Almufadi, "Fabrication and characterization of silicone rubber/multiwalled carbon nanotubes nanocomposite sensors under impact force" Sensors and Actuators A, 297, 111479 (2019).

26. X. Shi, B. Jiang, J. Wang, Y. Yang, Influence of wall number and surface functionalization of carbon nanotubes on their antioxidant behavior in high density polyethylene, Carbon 50 (2012) 1005–1013.
27. S. Yamane, S. Ata, L. Chen, H. Sato, T. Yamada, K. Hata, J. Mizukado, Experimental analysis of stabilizing effects of carbon nanotubes (CNTs) on thermal oxidation of poly(ethylene glycol)-CNT composites, Chem. Phys. Lett. 670 (2017) 32–36.
28. S. Ata, Y. Hayashi, T.B. Nguyen Thi, S. Tomonoh, S. Kawauchi, T. Yamada, K. Hata, Improving thermal durability and mechanical properties of poly(ether ether ketone) with single-walled carbon nanotubes, Polymer 176 (2019) 60–65.
29. A. Thabet, and N. Salem, "Experimental verification on dielectric breakdown strength using individual and multiple nanoparticles in polyvinyl chloride" Transactions on Electrical and Electronic Materials Journal, Vol.21, No.3, pp. 274-282, 2020.
30. Ahmed Thabet Mohamed, "Design and Investment of High Voltage NanoDielectrics" IGI Global, Publisher of Timely Knowledge, ISBN13: 9781799838296, ISBN10: 1799838293, EISBN13: 9781799838302, DOI: 10.4018/978-1-7998-3829-6, Pages 363, August 2020.
31. A. Thabet, and N. Salem, "Experimental Investigation on Dielectric Losses and Electric Field Distribution inside Nanocomposites Insulation of Three-Core Belted Power Cables" Advanced Industrial and Engineering Polymer Research, Vol.4, Issue 1, pp. 1857-1864, 2021.
32. A. Thabet, M. Fouad, "Assessment of Dielectric Strength and Partial Discharges Patterns in Nanocomposites Insulation of Single-Core Power Cables" Journal of Advanced Dielectrics (JAD), Vol.11, No.4, pp. 2150022 (1-10), 2021.
33. Ahmed Thabet Mohamed, "Emerging Nanotechnology Applications in Electrical Engineering" IGI Global, Publisher of Timely Knowledge, ISBN13: 9781799885368, ISBN10: 1799885364, EISBN13: 9781799885382, ISBN13 Softcover: 9781799885375, DOI: 10.4018/978-1-7998-8536-8, Pages 318, June 2021.